Toxicology in Vitro 30 (2015) 421–428

Contents lists available at ScienceDirect

Toxicology in Vitro

journal homepage: www.elsevier.com/locate/tiv

Protection against oxidative damage in human erythrocytes and preliminary photosafety assessment of *Punica granatum* seed oil nanoemulsions entrapping polyphenol-rich ethyl acetate fraction

Thaisa Baccarin [a,b], Montserrat Mitjans [a], Elenara Lemos-Senna [b], Maria Pilar Vinardell [a,*]

[a] Departament de Fisiologia, Facultat de Farmàcia, Universitat de Barcelona, Av. Joan XXIII s/n, E-08028 Barcelona, Spain
[b] Programa de Pós-Graduação em Farmácia, Centro de Ciências da Saúde, Universidade Federal de Santa Catarina, Campus Universitário Trindade, 88040-970 Florianópolis, SC, Brazil

ARTICLE INFO

Article history:
Received 16 April 2015
Received in revised form 18 September 2015
Accepted 20 September 2015
Available online 25 September 2015

Keywords:
Punica granatum
Seed oil
Polyphenol-rich ethyl acetate fraction
Fluorescent probes
Haemolysis
Photohaemolysis

ABSTRACT

The main purpose of the present study is to evaluate the ability of nanoemulsion entrapping pomegranate peel polyphenol-rich ethyl acetate fraction (EAF) prepared from pomegranate seed oil and medium chain triglyceride to protect human erythrocyte membrane from oxidative damage and to assess preliminary *in vitro* photosafety. In order to evaluate the phototoxic effect of nanoemulsions, human red blood cells (RBCs) are used as a biological model and the rate of haemolysis and photohaemolysis (5 J cm^{-2} UVA) is assessed *in vitro*. The level of protection against oxidative damage caused by the peroxyl radical generator AAPH in human RBCs as well as its effects on bilayer membrane characteristics such as fluidity, protein profile and RBCs morphology are determined. EAF-loaded nanoemulsions do not promote haemolysis or photohaemolysis. Anisotropy measurements show that nanoemulsions significantly retrain the increase in membrane fluidity caused by AAPH. SDS-PAGE analysis reveals that AAPH induced degradation of membrane proteins, but that nanoemulsions reduce the extension of degradation. Scanning electron microscopy examinations corroborate the interaction between AAPH, nanoemulsions and the RBC membrane bilayer. Our work demonstrates that *Punica granatum* nanoemulsions are photosafe and protect RBCs against oxidative damage and possible disturbance of the lipid bilayer of biomembranes. Moreover it suggests that these nanoemulsions could be promising new topical products to reduce the effects of sunlight on skin.

1. Introduction

The peel extract of *Punica granatum*, popularly known as pomegranate, contains a large quantity of phenolic compounds such as ellagic acid, gallic acid, punicalagin, punicalin, and luteolin (Amakura et al., 2000; Seeram et al., 2005; Van Elswijk et al., 2004). Pomegranate seed oil (PSO) contains conjugated fatty acids, in which the main constituent is punicic acid (El-Nemr et al., 2006; Fadavi et al., 2006), that it has been reported to have antioxidant properties (Qu et al., 2010). Phenolic compounds are natural antioxidants and are candidates for the ultraviolet photoprotection and prevention of ultraviolet radiation-induced oxidative stress and skin alteration, especially given their capacity to reduce the production of radicals, and their ability to stabilize reactions induced by oxygen and its radical species (González et al., 2013); promising applications of polyphenols exist in the cosmetic and pharmaceutical industries.

In a previous study, we developed PSO and medium chain triglyceride (MCT) nanoemulsion entrapping a pomegranate polyphenol-rich ethyl acetate fraction (EAF) for UV photoprotection application. Nanoemulsions (NEs) have attracted considerable attention for cosmetic and personal care as potential vehicles for releasing and improving the permeation of active compounds through the skin (Guglielmini, 2008). The *in vitro* antioxidant activity of free EAF and NE loaded with EAF (EAF-PSO-NE and EAF-MCT-NE) was confirmed using the ferric reducing antioxidant power (FRAP) and 2,2-diphenyl-1-picrylhydrazyl (DPPH) methods (Baccarin and Lemos-Senna, 2014).

The assessment of the toxicity potential of new molecules and formulations for human use is fundamental and it has become imperative for the nonclinical toxicologist to establish new approaches for early screening of potential cosmetic and pharmaceutical product candidates (Ahuja and Sharma, 2014). In particular, phototoxicity is of increasing concern in dermatology because of the increased level of ultraviolet radiation reaching the earth from the sun (Onoue et al., 2009). Phototoxicity can be caused by several classes of pharmaceuticals and cosmetics, which have the potential to provoke photoirritant, photoallergic and photogenotoxic events in light-exposed tissues through oxidation and

* Corresponding author at: Departament de Fisiologia, Facultat de Farmàcia, Universitat de Barcelona, Av. Joan XXIII s/n, E-08028 Barcelona, Spain.
E-mail address: mpvinardellmh@ub.edu (M.P. Vinardell).

http://dx.doi.org/10.1016/j.tiv.2015.09.020
0887-2333/

chemical modification under exposure to sunlight (Stein and Scheinfeld, 2007; Elkeeb et al., 2012).

Although there is no single method that provides all the toxicity information required, and since different nanosized systems elicit different biological responses, during the process of determining and studying the toxicological behaviour of a sample a combination of assays is often required. *In vitro* haemolysis is one of these assays (Doktorovova et al., 2014) and evaluates the biocompatibility of nanodroplets and formulation components (*i.e.*, surfactants, lipid) (Schubert and Müller-Goymann, 2005; Söderlind and Karlsson, 2006) *via* the impact of their physico–chemical characteristics on human red blood cells (RBCs), which is evaluated by quantifying the release of haemoglobin (Arora et al., 2012).

Therefore, the aim of this work was to evaluate the potential protective effect of free EAF, unloaded and EAF-loaded NEs against oxidative damage caused by the peroxyl radical generator 2,2′-azobis (amidinopropane dihydrochloride) (AAPH) in human erythrocytes and also to identify any possible irritant reactions; the potential irritancy and photo irritancy were assessed by *in vitro* haemolysis and photohaemolysis, respectively. The erythrocyte was chosen as an *in vitro* model since its membrane is rich in polyunsaturated fatty acids, which are extremely susceptible to free radical-mediated peroxidation; besides, erythrocytes have no internal organelles and because they are the simplest cell model available, they are the most popular cell membrane system for verifying possible membrane interactions and are considered to be representative of the plasma membrane in general (Magalhães et al., 2009; Svetina et al., 2004). Oxidative damage of the erythrocyte membrane may cause its malfunctioning by altering its fluidity and protein profile, manifested by decreased reduction in cytoskeletal protein content (low-molecular-weight, LMW) and the production of high-molecular-weight (HMW) proteins (Flynn et al., 1983; Snyder et al., 1985) and abnormalities in erythrocyte shape (Yang et al., 2006). Since these events have been proposed as a general mechanism leading to the haemolysis involved in cell injury and death (Alvarez-Suarez et al., 2012), we also evaluated them after RBCs were incubated with treatments.

To the best of our knowledge, this is the first time that the protective effect against oxidative damage in human erythrocytes of NE entrapping *P. granatum* peel polyphenol-rich EAF prepared using PSO or MCT as oil phases and their preliminary photosafety have been assessed using the above mentioned assays.

2. Materials and methods

2.1. Materials

Polysorbate 80 (Tween 80®), 2,2′-Azobis(2-methyl-propionamidine) dihydro-chloride (AAPH), triethanolamine, hydrogen peroxide 30% (w/w), sodium azide, sodium dodecyl sulfate (SDS), Triton X-100 and glycine were purchased from Sigma-Aldrich (St. Louis, MO, USA). NaCl, Na_2HPO_4 and KH_2PO_4 were purchased from Merck (Darmstadt, Germany). Ethyl acetate, dichloromethane, acetic acid and methanol were obtained from Vetec® (Rio de Janeiro, Brazil). Pomegranate seed oil and pomegranate fruit peel dry extract were purchased from *Via* Farma (Sao Paulo, Brazil). Soy lecithin (Lipoid® S100) was from Lipoid AG (Steinhausen, Switzerland). Medium chain triglyceride was from Brasquim (Porto Alegre, Brazil). Fluorescent probes DPH (1,6-diphenyl-1,3,5-hexatriene) and TMA-DPH (1-(4-trimethylammonium phenyl)-6-phenyl-1,3,4-hexatriene *p*-toluenesulfonate) were purchased from Molecular Probes (Eugene, OR). Acrylamide PAGE 40%, methylenebisacrylamide 2%, TEMED, mercaptoethanol, ammonium persulfate and bromophenol blue used for SDS-PAGE were obtained from GE Healthcare Amersham Biosciences (Uppsala, Sweden). Finally, water was purified in a Milli-Q system (Millipore, Bedford, MA).

2.2. Methods

2.2.1. Ethyl acetate fraction (EAF)

The pomegranate polyphenol-rich ethyl acetate fraction (EAF) was obtained from a commercial pomegranate peel dried extract and characterized through a high performance liquid chromatography (HPLC) method and spectrophotometric method (Folin–Ciocalteu) as described in our previously work (Baccarin and Lemos-Senna, 2014). Briefly, the dried powder was extracted by 24 hour dynamic maceration with a 90:10 (v/v) methanol:water mixture. The extractive solution was evaporated under reduced pressure for solvent removal, and the precipitate was suspended with a 2% aqueous acetic acid solution. The resulting mixture was then partitioned with dichloromethane and ethyl acetate. After that, the pooled ethyl acetate fraction was evaporated under reduced pressure to dryness.

2.2.2. Preparation of nanoemulsions

EAF-loaded pomegranate seed oil nanoemulsion (EAF-PSO-NE) or EAF-loaded medium chain triglyceride nanoemulsion (EAF-MCT-NE) were prepared using an ultrasonic emulsification method followed by solvent evaporation or spontaneous emulsification method, respectively (Baccarin and Lemos-Senna, 2014). Briefly, for the EAF-PSO-NE, the ethyl acetate fraction (EAF) (0.5%; w/v), soy lecithin (0.4%; w/v) and PSO (2%; w/v) were dissolved in 10 mL of ethyl acetate. This ethyl acetate solution was slowly poured into 40 mL of a polysorbate 80 (2.1%; w/v) aqueous solution. The oil in water dispersion was sonicated for 3 min using an Ultrasonic Processor UP200S (Hielscher, Germany), adjusted to pH 5.0–6.5 with triethanolamine (2%; w/v) and then it was and kept under magnetic stirring for 24 h. The resulting nanoemulsion was evaporated under reduced pressure up to volume of 15 mL.

For the EAF-MCT-NE, 10 mL of an ethanolic solution containing EAF (0.5%; w/v), soy lecithin (0.4%; w/v), and MCT (1.8%, w/v) was poured into a 2.1% (w/v) polysorbate 80 aqueous solution under magnetic stirring and adjusted to pH 5.0–6.5 with triethanolamine (2%; w/v). The nanoemulsion was then evaporated under reduce pressure to eliminate the organic solvent and concentrated up to volume of 15 mL. All formulations were filtered through 8 μm quantitative filter paper. Unloaded PSO-NE and MCT-NE were prepared in the same manner.

2.2.3. Physicochemical characterization of nanoemulsions

The mean droplet size and zeta potential were determined by dynamic light scattering (DLS) and laser-Doppler anemometry, respectively, using a Zetasizer Nano Series (Malvern Instruments, Worcestershire, UK). The size analyses were performed at a scattering angle of 173°, after appropriated dilution of the samples in ultrapure water (Milli-Q®, Millipore, USA). For zeta potential analysis, the samples were diluted in Milli-Q® water and placed in electrophoretic cells where a potential of $\pm$150 mV was applied. The zeta potential values were calculated as mean electrophoretic mobility values by using Smoluchowski's equation.

2.2.4. Preparation of red blood cell suspensions

Blood samples were obtained from anesthetized rats by cardiac puncture or from healthy volunteers from the Blood Bank of “Hospital Clinic” (Barcelona, Spain). All procedures followed the ethical guidelines of the University of Barcelona. Red blood cells (RBCs) were isolated by centrifugation at 3000 rpm at 4 °C for 10 min, and washed three times in isotonic PBS containing 123.3 mM NaCl, 22.2 mM Na_2HPO_4 and 5.6 mM KH_2PO_4 in distilled water (pH 7.4).

2.2.5. Haemolysis assay

The membrane-lytic activity of EAF, NE and formulation components (polysorbate 80, lecithin, MCT and PSO) was determined through haemolysis assay. A 25 μL aliquot of rat or human erythrocyte

suspension was exposed to each sample at various concentrations: EAF (10–1000 μg mL^{-1}), polysorbate 80 (0.5–80 mg mL^{-1}), lecithin (0.1–10 mg mL^{-1}), MCT (1–55 mg mL^{-1}), PSO (1–60 mg mL^{-1}), unloaded (MCT-NE and PSO-NE) and EAF-loaded nanoemulsions (EAF-MCT-NE and EAF-PSO-NE) (5–500 μg mL^{-1}) diluted in PBS solution in a total volume of 1 mL. Negative and positive controls were prepared by resuspending erythrocyte in buffer alone or distilled water, respectively. The samples were incubated at room temperature under constant shaking for 10 min, and then centrifuged at 10,000 rpm for 5 min. The absorbance of the haemoglobin released in the supernatant was measured at 540 nm using a Shimadzu UV-160A spectrophotometer (Shimadzu, Kyoto, Japan), and the percentages of haemolysis were obtained by comparing the sample absorbance with the positive control (totally haemolysed). Dose–response curves were plotted from haemolysis results and the concentrations inducing 50% haemolysis (HC_{50}) were calculated (Nogueira et al., 2012a).

2.2.6. Haemolysis induced by H_2O_2

The haemolysis induced by H_2O_2 was measured as reported by Ugartondo et al. (2009) with modifications. First, 250 μL of the human erythrocyte suspension, previously incubated with sodium azide (2 mM), was mixed with various concentrations of EAF (25–150 μg mL^{-1}), EAF-MCT-NE (25–100 μg mL^{-1}), EAF-PSO-NE (50–200 μg mL^{-1}). Then H_2O_2 was added and the mixture incubated for 90 min at 37 °C under stirring. The volume of each sample was adjusted to 1 mL with PBS. After final incubation, the samples were centrifuged at 10,000 rpm for 5 min, the supernatant was diluted 1:10 in PBS and the absorbance of the haemoglobin released was measured at 540 nm using a Shimadzu UV-160A spectrophotometer (Shimadzu, Kyoto, Japan). The percentages of haemolysis were obtained by comparing the sample absorbance with the positive control (totally haemolysed). The concentration inhibiting 50% of the haemolysis caused by H_2O_2 (IC_{50}) was determined for each sample. The experiment was carried out three times using three replicate samples for each sample concentration tested.

2.2.7. Photohaemolysis assay

Twenty-five microliter of rat or human red blood cell suspension were added to a 24-well plate containing 500 μg mL^{-1} of EAF, EAF-MCT-NE, EAF-PSO-NE, MCT-NE or PSO-NE. Then, one plate was exposed to UVA (TL-D 15 W/10 UVA lamp, Royal Philips Eletronics-The Netherlands) and the other was kept in the dark. Irradiance was measured using a Delta OHM photoradiometer (HD2302-Italy) to determine the time of exposure, using the formula:

$$E\left(J/cm^2\right) = t(s) \times P\left(W/cm^2\right) \quad (1)$$

where E is UV dose, t is the time expressed in seconds and, finally, P is the lamp potency. Cells were irradiated with 1.6–2.1 mW/cm^2 to give a final exposure of 5 J cm^2.

After irradiation the contents of each well were transferred to a tube and centrifuged at 1000 rpm for 5 min. The absorbance of the supernatant was measured at 525 nm using a Shimadzu UV-160A spectrophotometer (Shimadzu, Kyoto, Japan). The HC_{50} was determined for plates exposed and non-exposed to the UVA irradiation. The photohaemolysis factor (PHF) was calculated by dividing the HC_{50} of the non-irradiated cells by the HC_{50} of the irradiated cells. The haemoglobin oxidation assay measured the formation of intracellular and extracellular methaemoglobin. The same assay conditions as those of the photohaemolysis assay were used, except that 100 μL of Triton X-100 1% (v/v) solution was added to each irradiated and non-irradiated well and the absorbance of methaemoglobin was measured at 630 nm. The amount of methaemoglobin in the sample was determined by the difference in optical density (ΔOD) between the irradiated and non-irradiated plate. A product is considered photoirritant if the PHF is ≥3.0 or if the ΔOD is ≥0.05 (Pape et al., 2001).

2.2.8. Haemolysis mediated by AAPH

The haemolysis mediated by AAPH followed a method previously described in the literature, with some modifications (Miki et al., 1987). The addition of AAPH (a peroxyl radical initiator) to the human erythrocyte suspension induces the oxidation of cell membrane lipids and proteins, resulting in haemolysis. Aliquots of 83 μL of the human erythrocyte suspension were incubated with AAPH at a final concentration of 50 mM for 2.5 h in a shaker at 37 °C to achieve 100% haemolysis. The antihaemolytic activity of EAF (0.5–50 μg mL^{-1}), MCT-NE (5–100 μg mL^{-1}), EAF-MCT-NE (5–100 μg mL^{-1}), PSO-NE (5–100 μg mL^{-1}) and EAF-PSO-NE (5–100 μg mL^{-1}) was tested by adding several concentrations of each sample to the erythrocyte suspension in the presence of AAPH. A negative control (erythrocyte suspension with PBS alone) was included in all experiments to monitor spontaneous haemolysis. Samples plus erythrocyte suspension were also incubated without AAPH to determine whether the sample alone could cause haemolysis during 2.5 h of incubation. After incubation, the samples were centrifuged at 10,000 rpm for 5 min and the absorbance of the supernatant was measured at 540 nm in a Shimadzu spectrophotometer. The concentration inhibiting 50% of the haemolysis (IC_{50}) was determined for each sample.

2.2.9. Scanning electron microscopy — SEM

After 2.5 h of incubation, unwashed samples were fixed by adding 1 mL of 5.0% glutaraldehyde in PBS solution and incubated at 4 °C for 2 h. The samples were then centrifuged (1500 rpm for 10 min), the supernatant was discarded, and 1 mL of 2.5% glutaraldehyde in PBS was added. Fixed samples were washed with PBS solution, post-fixed with 1% osmium tetroxide, placed over a glass coverslip, dehydrated in an ascending series of ethyl alcohol (50–100%), air-dried using the critical point drying method in a CPD 7501 apparatus (Polaron, Watford, UK), and finally mounted on an aluminium stub and gold-coated in an SEM coating system SC 510 (Fisons Instruments, East Grinstead, UK). The resulting specimens were examined in a Zeiss DSM 940A scanning electron microscope (Carl Zeiss SMT AG, Jena, Germany).

2.2.10. Erythrocyte ghost preparation

After treatments and incubation for 2.5 h, human erythrocyte ghost membranes were prepared following the procedure proposed by Fairbanks (Fairbanks et al., 1971). Samples were centrifuged and the erythrocyte pellet was resuspended and washed with buffer (Na_2HPO_4 5 mM, pH 8.0) several times until white ghost membranes were obtained. The protein content of erythrocytes ghost cell membranes was measured using the Bio-Rad assay (Bio-Rad, Hercules, CA), which is based on the dye-binding procedure of Bradford (Bradford, 1976), using bovine serum albumin (BSA) as a protein standard.

2.2.11. SDS-PAGE

Sodium dodecyl sulfate-polyacrylamine gel electrophoresis of membrane proteins was performed according to Miki and collaborators (Miki et al., 1987) using a Mini-PROTEAN Tetra Cell unit (Bio-Rad, Hercules, CA). Erythrocyte ghost membranes were mixed with SDS sample buffer, heated at 95 °C for 5 min and then a total of 25 μg of protein was electrophoresed in parallel into 12.5% SDS-polyacrylamide gel under reducing conditions (slab gel consisted of 7.5% polyacrylamide resolving gel and 5% polyacrilamide stacking gel). Electrophoresis was carried out at 60 V for 10 min followed by 35 min at 200 V. Protein bands were viewed by staining with Coomassie brilliant blue R-250 for 50 min under gentle shaking and destained with a mixture of 7.5% methanol and 10% acetic acid. The molecular weight of the membrane proteins was estimated from the molecular size marker (Bio-Rad Precision Plus Unstained Standard), ranging from 10 to 250 kDa. Electrophoresis gel was digitized on a computer through a video camera. Thereafter, ImageJ software was used to calculate the average pixel intensity of bands 1, 2, 3, 4.1, 4.2 and 5 within regions of interest (ROI)

drawn on the collected gel images. Bands colour intensity was measured in triplicate for each treatment. The results were expressed as percentage of band colour intensity compared with control (100%) (Nogueira et al., 2012b).

2.2.12. Cell membrane fluidity

To determine cell membrane fluidity, fluorescence anisotropy measurements were carried out using DPH and TMA-DPH fluorescent probes (Nogueira et al., 2012b). Treated and non-treated human red blood cells suspensions (haematocrit of 0.01%) in PBS were labelled with the fluorescent probes (final concentration in samples 10^{-6} M) at room temperature for 1 h in dark conditions. Changes in membrane fluidity were also evaluated in samples incubated without AAPH to determine whether treatment alone can interfere in cell membrane fluidity. Steady-state anisotropy was measured using an SLM-Amino AB-2 spectrofluorometer, with polarizers in the L configuration in a quartz cuvette at room temperature. Samples were illuminated with linearly (vertically or horizontally) polarized monochromatic light (λ_{ex} = 365 nm), and the fluorescence intensities (λ_{em} = 425 nm), emitted parallel or perpendicular to the direction of the excitation beam (slit widths of 8 nm), were recorded. Fluorescence anisotropy (r) was calculated automatically by software provided with the instrument, according to the following equation:

$$r = \frac{(\mathrm{Ivv} - \mathrm{Ivh} \times \mathrm{G})}{(\mathrm{Ivv} + 2\mathrm{Ivh} \times \mathrm{G})} \quad (2)$$

where I_{vv} and I_{vh} represent the components of the light intensity emitted in parallel and perpendicular, respectively, to the direction of the vertically polarized excitation light. The factor $G = I_{hv}/I_{hh}$ was used to correct the inequality of the detection beam to horizontally and vertically polarized emission.

2.2.13. Statistical analysis

Each assay was carried out on three independent experiments using three replicate samples for each sample concentration tested. Statistical analyses were performed using one-way analysis of variance (ANOVA) followed by Dunnett's or Tukey's post-hoc test for multiple comparisons using GraphPad Prism 5.0 software. Differences were considered significant for $p < 0.05$ and $p < 0.001$.

3. Results

3.1. Physicochemical characterization of the nanoemulsions

It is important to determine the physicochemical characteristics of NE since these characteristics may not only alter the biological but also the toxicological response (Rivera Gil et al., 2010). Table 1 summarizes the physicochemical characteristics of unloaded and EAF-loaded NEs. The average size of all formulations, were about 200 nm, with the unloaded NE smaller than the loaded ones. The polydispersity indexes (PI) were <0.2, indicating that monodisperse colloidal dispersions were obtained. Zeta potential, which describes the surface charge of the NE droplets, varied from −20.1 to −24.7 mV, giving an indication of the physical stability of the colloidal dispersions (Mishra et al., 2009; Mitri et al., 2011).

Table 1
Physicochemical characterization of unloaded and EAF-loaded nanoemulsions.

Samples	Size (nm)	Zeta potential (mV)	Polydispersity index
EAF-PSO-NE	201.2 ± 3.8	−21.9 ± 2.2	0.17 ± 0.02
PSO-NE	180.7 ± 4.0	−20.1 ± 1.8	0.17 ± 0.01
EAF-MCT-NE	202.5 ± 1.3	−25.7 ± 4.0	0.11 ± 0.03
MCT-NE	186.5 ± 3.3	−22.3 ± 0.3	0.18 ± 0.01

Results are expressed as mean ± SD of at least 3 independent analyses.

3.2. Haemocompatibility and photohaemolysis studies

In the haemolysis assay the HC_{50} for the isolated formulations components was 7.25 ± 0.02 mg mL^{-1}, 1790 ± 1.83 mg mL^{-1}, 45.9 ± 0.07 mg mL^{-1}, 15.37 ± 0.54 mg mL^{-1} and >1 mg mL^{-1}, for soy lecithin, polysorbate 80, PSO, MCT and free EAF, respectively; for EAF-loaded nanoemulsions (EAF-PSO-NE; EAF-MCT-NE) and unloaded nanoemulsions (PSO-NE; MCT-NE) was >0.5 mg mL^{-1}. When the RBCs were irradiated, the EAF-loaded NEs (EAF-PSO-NE; EAF-MCT-NE) did not demonstrate a photohaemolitic behaviour.

3.3. Haemolysis mediated by H_2O_2 and AAPH

After verifying the haemolytic capacity of EAF and EAF-loaded NEs, their capacity to protect human RBCs against haemolysis induced by H_2O_2 and AAPH was evaluated (Fig. 1).

Oxygen free radicals are implicated in many biological processes and for the most part, the endogenous antioxidant system can manage their detoxification. However, certain external events can trigger the production of these damaging free radicals. Hydroxyl ($OH^{\bullet}$) and superoxide ($O_2^{\bullet -}$) free radical are two oxygen free radical species in biological systems. Normally, the enzymes catalase, superoxide dismutase, and glutathione peroxidase maintain these free radicals at low levels, but under certain circumstances, higher levels of these compounds may be available, thus leading to oxidative damage (Floyd and Lewis, 1983).

Hydrogen peroxide is generated by the dismutation of superoxide radical, catalysed by superoxide dismutase enzymes and directly produced by oxidase enzymes. It can lead the production of hydroxyl free radicals either by exposure to ultraviolet light or by interaction with transition metal ions, mostly iron (Fenton-type reaction) (Halliwell et al., 2000). Also, hydrogen peroxide may enter the human body through skin contact; it crosses the RBC lipid membrane and acts on the intracellular moiety, forming hydroxyl radicals that can initiate lipid peroxidation and cause cell damage (Alam et al., 2013; Blasa et al., 2007). In the case of haemolysis induced by H_2O_2 the IC_{50} of EAF and EAF-MCT-NE did not differ significantly, being 31.62 and 27.16 μg mL^{-1}, respectively; EAF-PSO-NE presented a slightly higher IC_{50}, at 76.05 μg mL^{-1}. During AAPH-induced haemolysis the EAF showed an IC_{50} of 1.20 μg mL^{-1} which places it at the same level of two well-known antioxidants, ascorbic acid IC_{50} 7.5 μg mL^{-1} (Aman et al., 2013) and curcumin IC_{50} 2.94 μg mL^{-1} (Banerjee et al., 2008). In the absence of AAPH, RBCs were stable and haemolysis was negligible (data not shown). The percentage of haemolysis in RBCs incubated only with EAF or EAF-loaded NEs was almost identical to that of the

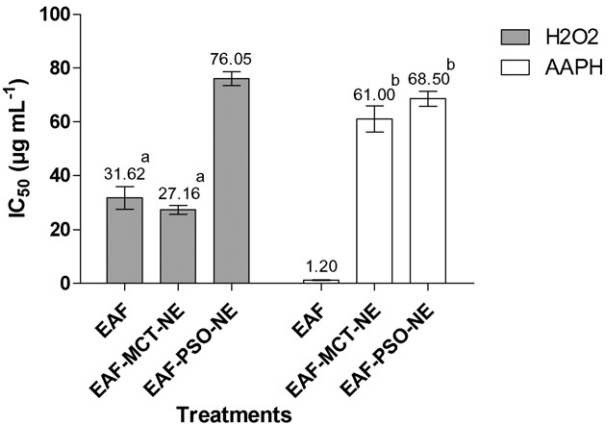

Fig. 1. Protective effect of *P. granatum* EAF and EAF-loaded nanoemulsions against oxidative haemolysis induced by H_2O_2 and AAPH. Results are expressed as mean ± SEM of at least 3 independent assays. Statistical analyses were performed by ANOVA followed by Tukey's multiple comparison test ($p < 0.05$). Same letters mean no statistical difference.

control sample (RBCs + PBS) indicating that EAF and EAF-loaded NEs themselves do not induce haemolysis.

3.4. Erythrocyte membrane fluidity

Table 2 shows the anisotropy values for both probes after AAPH assay. An increase in the *r* values (anisotropy measurement) of a probe is indicative of a decrease in the fluidity of the membrane. The baseline fluorescence for DPH and TMA-DPH was 0.2404 ± 0.0059 and 0.2456 ± 0.0065, respectively. Free EAF and EAF-loaded NEs containing PSO (EAF-PSO-NE) or MCT (EAF-MCT-NE) maintained the fluidity in the outer and inner parts of erythrocytes membranes at around baseline levels (control PBS). The presence of AAPH alone increased anisotropy values, indicating a decrease in membrane fluidity. In AAPH-induced peroxidation, free radicals are formed in the solution and attack the membranes from the external medium forming lipid hydroperoxides (Arora et al., 2012). Co-incubated free EAF or EAF-loaded NEs managed to retrain the fluidity diminution caused by AAPH, suggesting that the polyphenols present in the EAF stop the free radicals attacking and accessing the bilayer.

3.5. SDS-PAGE

Given the changes in membrane fluidity, the next step was to run an SDS-PAGE experiment to assess possible changes in membrane proteins in human erythrocytes. Oxidants basically alter the erythrocyte membrane by decreasing the LMW proteins and producing HMW proteins (Flynn et al., 1983; Snyder et al., 1985). Fig. 2 shows the electrophoretic profile of the erythrocyte membrane proteins.

When RBCs were incubated with EAF or NE alone, the level of in erythrocyte-membrane proteins was maintained at a background level similar to that in the untreated samples (control) (data not shown). The well-established normal distribution of the major membrane cytoskeletal proteins is shown in lane 2, which contains untreated erythrocytes ghosts. AAPH treatment produced changes in the protein pattern, leading to a remarkable loss of spectrins (band 1 and 2), and band 3, 4.1, 4.2 and 5, as seen in lane 3, confirming previous results from other authors (Hseu et al., 2002; Martínez et al., 2012; Yang et al., 2006). As shown in lanes 4, 5 and 6, the analysis of LMW proteins revealed that EAF and EAF-loaded NEs protected against AAPH-induced changes in the amount of erythrocytes membrane proteins. Table 3 shows the results expressed as the percentage of band colour intensity compared with the control (100%).

After AAPH treatment, the amount of band 1, 2, 3, 4 and 5 proteins dropped to 37%, 40%, 5% and 23%, respectively, in comparison with untreated erythrocytes. On the other hand, the co-treatment of erythrocytes with AAPH and EAF or EAF-loaded NEs containing PSO (EAF-PSO-NE) or MCT (EAF-MCT-NE) as the oil phase, reduced the effects of the oxidant agent on those proteins. This reduction was better and more evident when the EAF was nanoemulsified (EAF-PSO-NE or EAF-MCT-NE).

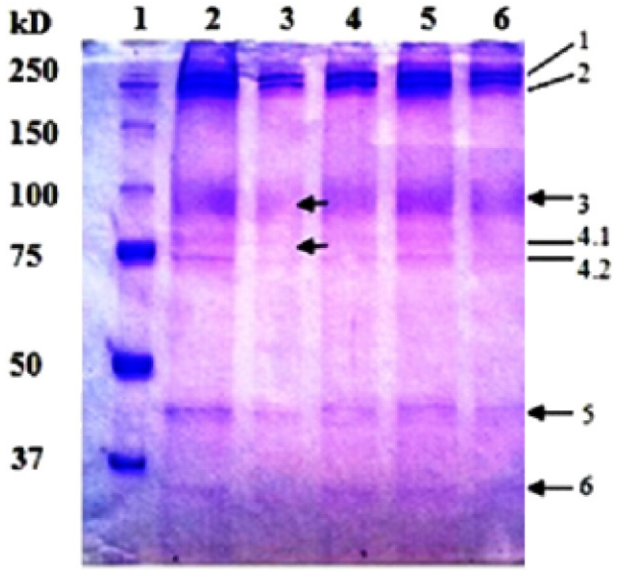

Fig. 2. Protective effect of *P. granatum* EAF and EAF-loaded nanoemulsions for human erythrocyte membrane skeletal proteins after incubation with AAPH, determined by SDS-PAGE. Following preincubation of the erythrocytes for 2.5 h in the absence or presence of AAPH and treatments, membranes were separated and washed as described in Section 2.2.12. The major cytoskeletal protein bands are identified following the classification of Fairbanks et al. (1971) and are given on the right of the gel. Each lane corresponds to a different treatment: (1) protein standard; (2) control PBS (untreated membrane); (3) AAPH control; treatment with ethyl acetate fraction and nanoemulsions in the presence of AAPH (4) EAF (1 μg mL^{-1}), (5) EAF-PSO-NE (50 μg mL^{-1}), (6) EAF-MCT-NE (50 μg mL^{-1}).

3.6. SEM analysis

The protein organization network found mainly in the inner membrane layer is responsible for the maintenance of shape and stability; once the protein network is compromised the shape of the erythrocyte may change (Vittori et al., 2002). As mentioned previously, oxidative damage in cell membranes leads to changes in the protein profile. The effect of AAPH alone, EAF and EAF-loaded NEs co-incubated with AAPH on erythrocyte morphology was studied by SEM analysis (Fig. 3).

SEM examinations corroborated that AAPH, nanoemulsions and the EAF interacted with the lipid bilayer by altering the normal morphology of the RBCs. Treatment of erythrocytes with AAPH alone resulted in a significant change in shape to echinocytic or acanthocytic (Fig. 3A). In our study the control erythrocytes incubated with PBS solution for 2.5 h presented a leptocyte-type shape (Fig. 3B-1), *i.e.*, a flattened cell with reduced volume; assuming that the long incubation time was somehow deforming the RBCs, SEM preparation was then conducted immediately after adding RBCs to the PBS solution, but the findings were the same (Fig. 3B-2); it is thus likely that this was a blood sample characteristic. EAF (Fig. 3C) and EAF-loaded NEs (Fig. 3D) incubated with AAPH showed the knizocyte and stomatocyte-type deformation; knizocyte is a cell with two or three concavities while a stomatocyte is a cell with one concavity in the shape of a mouth. The EAF and EAF-loaded NEs incubated with RBCs alone did not alter the morphology of the erythrocytes that remained as the control ones (data not shown).

Table 2
Steady-state fluorescence anisotropy of the probes DPH and TMA-DPH incorporated into erythrocyte membrane after AAPH assay.

Samples (μg mL^{-1})	(r^*) DPH (mean ± SE)	(r^*) TMA-DPH (mean ± SE)
Control	0.2404 ± 0.0059	0.2456 ± 0.0065
AAPH (50 mM)	0.3427 ± 0.0069**	0.3315 ± 0.0053**
EAF (1)	0.2488 ± 0.0060***	0.2465 ± 0.0064***
[a]EAF (1)	0.2351 ± 0.0073***	0.2534 ± 0.0066***
EAF-MCT-NE (50)	0.2498 ± 0.0060***	0.2489 ± 0.0059***
[a]EAF-MCT-NE (50)	0.2465 ± 0.0058***	0.2443 ± 0.0060***
EAF-PSO-NE (50)	0.2329 ± 0.0058***	0.2382 ± 0.0052***
[a]EAF-PSO-NE (50)	0.2449 ± 0.0079***	0.2496 ± 0.0076***

Data represent the means of three independent experiments ± SE, each conducted in triplicate.
[a] Samples incubated without AAPH.
* *r* values = anisotropy measurements.
** $p < 0.01$ when compared to control PBS (Dunnett's post hoc test).
*** $p < 0.01$ when compared to AAPH (Dunnett's post hoc test).

Table 3
Effect of AAPH and EAF and EAF-loaded nanoemulsions (EAF-PSO-NE and EAF-MCT-NE) on protein bands of human erythrocyte membrane.

Treatment	Band 1 and 2	Band 3	Band 4.1 and 4.2	Band 5
AAPH 50 Mm	37.42 ± 1.45*	39.65 ± 2.42*	4.96 ± 4.97*	22.94 ± 1.06*
AAPH + EAF 1 μg mL^{-1}	59.28 ± 2.05**a	70.03 ± 4.32**b	32.63 ± 3.49**	50.43 ± 1.01**
AAPH + EAF-PSO-NE 50 μg mL^{-1}	81.08 ± 1.24**	88.02 ± 4.47**c	61.10 ± 3.40**d	69.08 ± 0.85**e
AAPH + EAF-MCT-NE 50 μg mL^{-1}	60.35 ± 1.90**a	75.29 ± 4.18**b,c	59.49 ± 2.42**d	65.80 ± 0.45**e

The results are expressed as percentage of control taking control as 100%. Values are mean ± SEM of three experiments. See the Materials and methods section for details of the analysis performed. Statistical analyses were performed by ANOVA followed by Tukey's multiple comparison tests (same letter means no statistical difference).
* Significant difference from control group ($p < 0.01$).
** Significant difference from AAPH group $p < 0.01$).

4. Dicussion

P. granatum is well known for its considerable polyphenolics content; they are bioactive secondary metabolites widely distributed in plants (Harborne, 1989) and contain one or more aromatic hydroxyl groups that actively scavenge free radicals and are responsible for antioxidant activity. It is essential to identify and quantify the polyphenolic compounds in both free EAF and EAF-loaded NEs, given that their capacity to protect erythrocytes against oxidation is largely related to the characteristics of these compounds. EAF contains at least 600 mg g^{-1} GAE (gallic acid equivalents) of total phenolic content, among which ellagic acid, gallic acid, and punicalagin are the major ones (8.47%, 23.86% and 29.67% w/w, respectively). The nanoemulsions presented entrapment efficiency near or above 50% depending on the chemical compound lipophilicity. Details of the polyphenol identification and quantification through HPLC method are described in a previous study (Baccarin and Lemos-Senna, 2014).

Haemocompatibility testing, a major part of biocompatibility testing, comprises the evaluation of interactions of foreign material such as active compounds, excipients and/or formulations with human red blood cells and to explore possible damaging effects arising from these combined exposure (Szebeni, 2012). Haemolysis of human RBCs is a very good model not only for studying free radical induced oxidative damage to membranes and to evaluate the antioxidant activity of new compound or formulation, but also to determine the topical irritation and/or phototoxic potential (photohaemolysis) of these substances (Pape and Hoppe, 1991; Pape et al., 1987). With respect to the potential topical application of EAF-loaded NEs as a photoprotector and according to the Safety Evaluation Guide for Cosmetic Products (Brasil, 2003) it is extremely important to evaluate their potential topical irritation and photoirritation. Some studies have reported the photohaemolytic potential of hydroalcoholic extracts (Madariaga et al., 2010; Toledo et al., 2012). Nevertheless, there are few studies in the literature related to the effects of nanodispersions (*i.e.*, nanoemulsion) and even fewer related to nanoemulsions loaded with plant extracts or extract fractions.

Several studies support the use of RBCs as a model of oxidative damage induced by AAPH (Ajila and Prasada Rao, 2008; Alvarez-Suarez et al., 2012; Banerjee et al., 2008; Blasa et al., 2007; Botta et al., 2014; Chirinos et al., 2008; Hseu et al., 2002; Magalhães et al., 2009; Martínez et al., 2012; Yang et al., 2006). When AAPH is added as a radical initiator, it decomposes at physiological temperature in aqueous solution to generate alkyl radicals, which in the presence of oxygen are converted to the corresponding peroxyl radicals; in turn, these peroxyl radicals induce oxidation of polyunsaturated lipids in the RBCs membrane, causing a chain reaction known as lipid peroxidation (Banerjee et al., 2008).

Both EAF and EAF-loaded NEs demonstrated antioxidant properties against oxidative damage in the erythrocyte membrane induced by H_2O_2 or AAPH. The different IC_{50} values obtained for the H_2O_2 and AAPH assays only emphasizes the fact that conclusions about antioxidant activity should not be based on a single test model, because each assay represents a different type of oxidative damage and varies in different respects; therefore samples may also behave differently. With regard to AAPH assay, it was observed that the NE presented a higher IC_{50} than the free EAF, which can be explained by the fact that as the EAF is encapsulated it is not totally available in the assay medium in order to directly neutralize the peroxyl radicals generated from AAPH.

The incorporation of EAF and NE into RBCs could cause conformational alterations in membrane cytoskeletal proteins and changes in the internal viscosity of the cells. To determine whether free EAF or

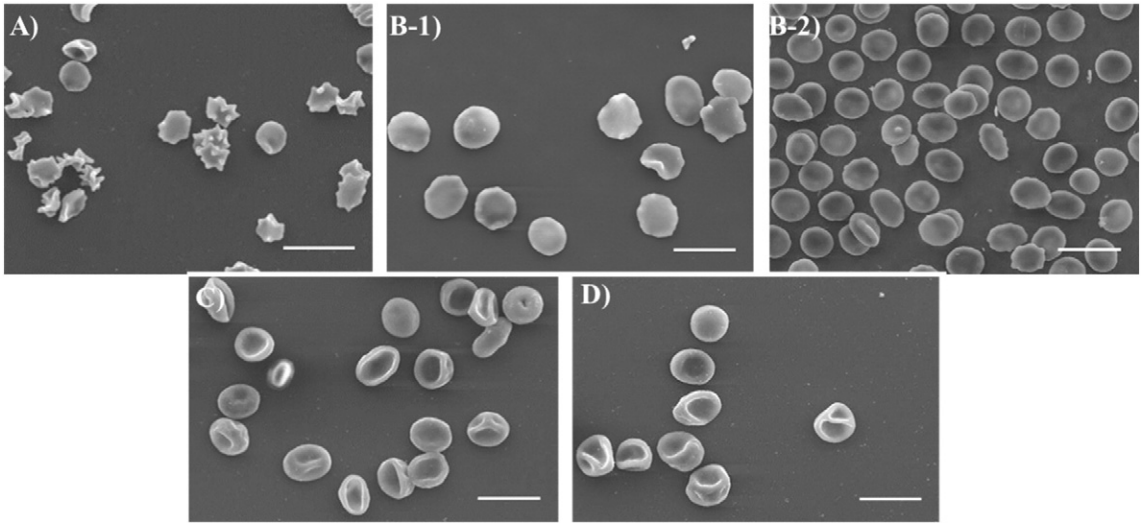

Fig. 3. Scanning electron micrograph of normal human erythrocyte and protective effects of ethyl acetate fraction (EAF) and nanoemulsions of *P. granatum* peel extract against AAPH induced oxidative damage on RBC. A) AAPH at 50 mM; B-1) Control in PBS and B-2) Control in PBS after 2.5 h incubation; C) EAF (1.5 μg mL^{-1}) with AAPH at 50 mM; D) EAF-loaded NEs (50 μg mL^{-1}) with AAPH at 50 mM. Scale bars correspond to 10 μm.

EAF-loaded NEs disturb the phospholipid bilayer across its thickness, steady-state fluorescence anisotropy (r) was measured to test membrane fluidity, as this is a sensitive indicator for monitoring fluorophore binding to regions of biomembranes with constrained movement (Hou et al., 2011; Nogueira et al., 2012b). This is an important parameter related to the structure and functional state of the cell membrane (Marczak, 2009).

The fluorescent probes, DPH and TMA-DPH, were incorporated into the human erythrocyte membranes to detect possible changes in membrane fluidity. DPH is incorporated within the hydrophobic region of the bilayer membrane, while TMA-DPH is incorporated near the surface of the cell membrane (Marczak, 2009). The fluorescence anisotropy values are inversely proportional to cell membrane fluidity. A high degree of fluorescence anisotropy, represents a high structural order and/or low cell membrane fluidity. Therefore, it is possible to assess the arrangement and mobility of membrane components in different regions of the bilayer (Marczak, 2009).

Our findings suggest that the possible localization of phenolic compounds of EAF-loaded NEs on the erythrocyte membrane is not restricted to one determined zone since EAF-loaded NEs when together with AAPH were able to elevate the fluidity of both the inner and outer layer, allowing better interaction between the antioxidant compounds and lipophilic radicals.

The degree of protection afforded by free EAF and EAF-loaded NEs against human erythrocyte oxidation might be attributed to different features. First, the partition coefficient or degree of lipophilicity of phenolic compounds determines their interaction with biomembranes and influences their antioxidant capacity and/or ability to interact with free radicals present in the aqueous medium of the oxidation system (Liao and Yin, 2000). Second, the chemical structure of the phenolic compounds determines their ability to react with free radicals; for phenolic acids, the free radical-scavenging properties depend mainly on their number of hydroxyl groups that have the ability to donate hydrogen, thereby forming a stable end-product, which does not initiate or propagate further oxidation of the lipid (Hsieh et al., 2005). Third, in phenolic mixtures *i.e.*, extract and/or extract fraction, the presence of synergism may modify the characteristics of oxidation inhibition (Chirinos et al., 2008).

Regarding the membrane protein profile, when the RBCs were treated with the EAF-loaded NEs (EAF-PSO-NE or EAF-MCT-NE) a more efficient protection against the oxidant agent on the membrane proteins was observed. This is probably due to the fact that one of the advantages of NE is that they better solubilize lipophilic compounds and enhance their transportation through lipid layers. In this way, it is not only the water-soluble radical scavengers present in the EAF that efficiently scavenge the peroxyl radicals in the medium before they attack the erythrocytes, but also the lipid-soluble ones which are located in lipophilic regions of the membrane (Blasa et al., 2007). Furthermore, EAF-PSO-NE appears to deliver an even better cell membrane protection, since PSO also presents antioxidants compounds that may act in a synergistic manner with EAF.

SEM studies corroborated the interaction of AAPH, EAF-PSO-NE and EAF-MCT-NE and free EAF with the lipid bilayer, as demonstrated by the changes in cell shape. According to the bilayer couple hypothesis, the shape changes induced in erythrocytes by foreign molecules are due to deferential expansion of the two monolayers of the RBCs membrane. Thus, stomatocytes are formed when the compound inserts into the inner monolayer, whereas speculated-shaped echinocytes are produced when it inserts into the outer moiety, causing surface expansion (Lim et al., 2002; Sheetz and Singer, 1974).

Finally, nanoemulsions entrapping pomegranate peel polyphenol-rich EAF have a great potential for cosmetic application as antioxidant and photoprotector. The present study indicates that EAF-PSO-NE and EAF-MCT-NE were photosafe in a preliminary *in vitro* test and protected the RBC membrane against oxidative damage.

Conflict of interest

The authors declare no competing financial interest.

Acknowledgments

The authors acknowledge financial support from CAPES (CAPES/PDSE project no. BEX 5613/13-2), the Ministerio de Economía y Competitividad-Spain (project MAT2012-38047-C02-01) and European Union (FEDER). The authors would like to thank Professor Dr. Lourdes Pérez for Malvern Zetasizer Nano ZS use and Professor Dr. Maria Antonia Busquets for SLM-Amino AB-2 Spectrofluorometer use.

References

Ahuja, V., Sharma, S., 2014. Drug safety testing paradigm, current progress and future challenges: an overview. J. Appl. Toxicol. 34, 576–594.
Ajila, C.M., Prasada Rao, U.J.S., 2008. Protection against hydrogen peroxide induced oxidative damage in rat erythrocytes by *Mangifera indica* L. peel extract. Food Chem. Toxicol. 46, 303–309.
Alam, M.N., Bristi, N.J., Rafiquzzaman, M., 2013. Review on in vivo and in vitro methods evaluation of antioxidant activity. Saudi Pharm. J. 21, 143–152.
Alvarez-Suarez, J.M., Giampieri, F., González-Paramás, A.M., Damiani, E., Astolfi, P., Martinez-Sanchez, G., Bompadre, S., Quiles, J.L., Santos-Buelga, C., Battino, M., 2012. Phenolics from monofloral honeys protect human erythrocyte membranes against oxidative damage. Food Chem. Toxicol. 50, 1508–1516.
Amakura, Y., Okada, M., Tsuji, S., Tonogai, Y., 2000. High-performance liquid chromatographic determination with photodiode array detection of ellagic acid in fresh and processed fruits. J. Chromatogr. A 896, 87–93.
Aman, S., Moin, S., Owais, M., Siddiqui, M.U., 2013. Antioxidant activity of thymol: protective role in AAPH-induced hemolysis in diabetic erythrocytes. Int. J. Pharm. Sci. Invent. 2, 55–60.
Arora, S., Rajwade, J.M., Paknikar, K.M., 2012. Nanotoxicology and in vitro studies: the need of the hour. Toxicol. Appl. Pharmacol. 258, 151–165.
Baccarin, T., Lemos-Senna, E., 2014. Pomegranate seed Oil nanoemulsions encapsulating pomegranate peel polyphenol-rich ethyl acetate fraction: development and antioxidant assessment. J. Nanopharmaceutics Drug Deliv. 2, 333–343.
Banerjee, A., Kunwar, A., Mishra, B., Priyadarsini, K.I., 2008. Concentration dependent antioxidant/pro-oxidant activity of curcumin: studies from AAPH induced hemolysis of RBCs. Chem. Biol. Interact. 174, 134–139.
Blasa, M., Candiracci, M., Accorsi, A., Piacentini, M.P., Piatti, E., 2007. Honey flavonoids as protection agents against oxidative damage to human red blood cells. Food Chem. 104, 1635–1640.
Botta, A., Martínez, V., Mitjans, M., Balboa, E., Conde, E., Vinardell, M.P., 2014. Erythrocytes and cell line-based assays to evaluate the cytoprotective activity of antioxidant components obtained from natural sources. Toxicol. In Vitro 28, 120–124.
Bradford, M.M., 1976. A rapid and sensitive method for the quantitation of microgram quantities of protein utilizing the principle of protein-dye binding. Anal. Biochem. 72, 248–254.
Brasil, 2003. Guia para avaliação de segurança de produtos cosméticos. Agência Nacional de Vigilância Sanitáriapp. 1–47.
Chirinos, R., Campos, D., Warnier, M., Pedreschi, R., Rees, J.-F., Larondelle, Y., 2008. Antioxidant properties of mashua (*Tropaeolum tuberosum*) phenolic extracts against oxidative damage using biological in vitro assays. Food Chem. 111, 98–105.
Doktorovova, S., Souto, E.B., Silva, A.M., 2014. Nanotoxicology applied to solid lipid nanoparticles and nanostructured lipid carriers — a systematic review of in vitro data. Eur. J. Pharm. Biopharm. 87, 1–18.
Elkeeb, D., Elkeeb, L., Maibach, H., 2012. Photosensitivity: a current biological overview. Cutan. Ocul. Toxicol 31, 263–272.
El-Nemr, S.E., Ismail, I.A., Ragab, M., 2006. Chemical composition of juice and seeds of pomegranate fruit. Die Nahrung 34, 601–606.
Fadavi, A., Barzegar, M., Azizi, H.M., 2006. Determination of fatty acids and total lipid content in oilseed of 25 pomegranates varieties grown in Iran. J. Food Compos. Anal. 19, 676–680.
Fairbanks, G., Steck, T.L., Wallach, D.F.H., 1971. Electrophoretic analysis of the major polypeptides of the human erythrocyte membrane. Biochemistry 10, 2606–2617.
Floyd, R.A., Lewis, A.C., 1983. Hydroxyl free radical formation from hydrogen peroxide by ferrous iron-nucleotide complexes. Biochemistry 22, 2645–2649.
Flynn, T.P., Allen, D.W., Johnson, G.J., White, J.G., 1983. Oxidant damage of the lipids and proteins of the erythrocyte membranes in unstable hemoglobin disease. Evidence for the role of lipid peroxidation. J. Clin. Invest. 71, 1215–1223.
González, N., Ribeiro, D., Fernandes, E., Nogueira, D.R., Conde, E., Moure, A., Vinardell, M.P., Mitjans, M., Domínguez, H., 2013. Potential use of *Cytisus scoparius* extracts in topical applications for skin protection against oxidative damage. J. Photochem. Photobiol. B 125, 83–89.
Guglielmini, G., 2008. Nanostructured novel carrier for topical application. Clin. Dermatol. 26, 341–346.
Halliwell, B., Clement, M.V., Long, L.H., 2000. Hydrogen peroxide in the human body. FEBS Lett. 486, 10–13.

Harborne, J.B., 1989. General procedures and measurements of total phenolics. In: Harborne, J.B. (Ed.), Methods in plant biochemistry. Plant phenolics. Academic Press, London.

Hou, S.-Z., Su, Z.-R., Chen, S.-X., Ye, M.-R., Huang, S., Liu, L., Zhou, H., Lai, X.-P., 2011. Role of the interaction between puerarin and the erythrocyte membrane in puerarin-induced hemolysis. Chem. Biol. Interact. 192, 184–192.

Hseu, Y.-C., Chang, W.-C., Hseu, Y.-T., Lee, C.-Y., Yech, Y.-J., Chen, P.-C., Chen, J.-Y., Yang, H.-L., 2002. Protection of oxidative damage by aqueous extract from Antrodia camphorata mycelia in normal human erythrocytes. Life Sci. 71, 469–482.

Hsieh, C.-L., Yen, G.-C., Chen, H.-Y., 2005. Antioxidant activities of phenolic acids on ultraviolet radiation-induced erythrocyte and Low density lipoprotein oxidation. J. Agric. Food Chem. 53, 6151–6155.

Liao, K.-l., Yin, M.-C., 2000. Individual and combined antioxidant effects of seven phenolic agents in human erythrocyte membrane ghosts and phosphatidylcholine liposome systems: importance of the partition coefficient. J. Agric. Food Chem. 48, 2266–2270.

Lim, H.W.G., Wortis, M., Mukhopadhyay, R., 2002. Stomatocyte–discocyte–echinocyte sequence of the human red blood cell: evidence for the bilayer-couple hypothesis from membrane mechanics. Proc. Natl. Acad. Sci. U. S. A. 99, 16766–16769.

Madariaga, Y.G., Cárdenas, M.B., Toledo, D.B., Alfonso, O.C., Montalbán, C.M.M., Bernal, Y.M., 2010. In vitro photohemolitic assessment of *Cissus sicyoides* L. and *Achyranthes aspera*. Rev. Cuba. Plant. Med. 15, 126–132.

Magalhães, A.S., Silva, B.M., Pereira, J.A., Andrade, P.B., Valentão, P., Carvalho, M., 2009. Protective effect of quince (*Cydonia oblonga* Miller) fruit against oxidative hemolysis of human erythrocytes. Food Chem. Toxicol. 47, 1372–1377.

Marczak, A., 2009. Fluorescence anisotropy of membrane fluidity probes in human erythrocytes incubated with anthracyclines and glutaraldehyde. Bioelectrochemistry 74, 236–239.

Martínez, V., Ugartondo, V., Vinardell, M.P., Torres, J.L., Mitjans, M., 2012. Grape epicatechin conjugates prevent erythrocyte membrane protein oxidation. J. Agric. Food Chem. 60, 4090–4095.

Miki, M., Tamai, H., Mino, M., Yamamoto, Y., Niki, E., 1987. Free-radical chain oxidation of rat red blood cells by molecular oxygen and its inhibition by α-tocopherol. Arch. Biochem. Biophys. 258, 373–380.

Mishra, A., Ram, S., Ghosh, G., 2009. Dynamic light scattering and optical absorption in biological nanofluids of gold nanoparticles in poly(vinyl pyrrolidone) molecules. J. Phys. Chem. C 113, 6976–6982.

Mitri, K., Shegokar, R., Gohla, S., Anselmi, C., Müller, R.H., 2011. Lipid nanocarriers for dermal delivery of lutein: preparation, characterization, stability and performance. Int. J. Pharm. 414, 267–275.

Nogueira, D., Mitjans, M., Morán, M.C., Pérez, L., Vinardell, M.P., 2012a. Membrane-destabilizing activity of pH-responsive cationic lysine-based surfactants: role of charge position and alkyl chain length. Amino Acids 43, 1203–1215.

Nogueira, D.R., Mitjans, M., Busquets, M.A., Pérez, L., Vinardell, M.P., 2012b. Phospholipid bilayer-perturbing properties underlying lysis induced by pH-sensitive cationic lysine-based surfactants in biomembranes. Langmuir 28, 11687–11698.

Onoue, S., Seto, Y., Gandy, G., Yamada, S., 2009. Drug-induced phototoxicity; an early in vitro identification of phototoxic potential of new drug entities in drug discovery and development. Curr. Drug Saf. 4, 123–136.

Pape, W.J.W., Hoppe, U., 1991. In vitro methods for the assessment of primary local effects of topically applied preparations. Skin Pharmacol. 4, 205–212.

Pape, W.J.W., Pfannenbecker, U., Hoppe, U., 1987. Validation of the red blood cell system as in vitro assay for rapid screening of irritation potential of surfactants. Mol. Toxicol. 1, 525–536.

Pape, W.J.W., Maurer, T., Pfannenbecker, U., Steiling, W., 2001. The red blood cell phototoxicity test (photohaemolysis and haemoglobin oxidation): EU/COLIPA validation programme on phototoxicity (phase II). ATLA. Altern. Lab. Anim. 29, 145–162.

Qu, W., Pan, Z., Ma, H., 2010. Extraction modeling and activities of antioxidants from pomegranate marc. J. Food Eng. 99, 16–23.

Rivera Gil, P., Oberdörster, G., Elder, A., Puntes, V., Parak, W.J., 2010. Correlating physicochemical with toxicological properties of nanoparticles: the present and the future. ACS Nano 4, 5527–5531.

Schubert, M.A., Müller-Goymann, C.C., 2005. Characterisation of surface-modified solid lipid nanoparticles (SLN): influence of lecithin and nonionic emulsifier. Eur. J. Pharm. Biopharm. 61, 77–86.

Seeram, N.P., Adams, L.S., Henning, S.M., Niu, Y., Zhang, Y., Nair, M.G., Heber, D., 2005. In vitro antiproliferative, apoptotic and antioxidant activities of punicalagin, ellagic acid and a total pomegranate tannin extract are enhanced in combination with other polyphenols as found in pomegranate juice. J. Nutr. Biochem. 16, 360–367.

Sheetz, M.P., Singer, S., 1974. Biological membranes as bilayer couples. A molecular mechanism of drug-erythrocyte interactions. Proc. Natl. Acad. Sci. U. S. A. 71, 4457–4461.

Snyder, L.M., Fortier, N.L., Trainor, J., Jacobs, J., Leb, L., Lubin, B., Chiu, D., Shohet, S., Mohandas, N., 1985. Effect of hydrogen peroxide exposure on normal human erythrocyte deformability, morphology, surface characteristics, and spectrin-hemoglobin cross-linking. J. Clin. Invest. 76, 1971–1977.

Söderlind, E., Karlsson, L., 2006. Haemolytic activity of maltopyranoside surfactants. Eur. J. Pharm. Biopharm. 62, 254–259.

Stein, K.R., Scheinfeld, N.S., 2007. Drug-induced photoallergic and phototoxic reactions. Expert Opin. Drug Saf. 6, 431–443.

Svetina, S., Kuzman, D., Waugh, R.E., Ziherl, P., Žekš, B., 2004. The cooperative role of membrane skeleton and bilayer in the mechanical behaviour of red blood cells. Bioelectrochemistry 62, 107–113.

Szebeni, J., 2012. Hemocompatibility testing for nanomedicines and biologicals: predictive assays for complement mediated infusion reactions. Eur. J. Nanomed. 4, 33–53.

Toledo, D.B., Cárdenas, M.B., Díaz, A.V., Montalbán, C.M.M., Rodriguez, N.I., 2012. Evaluación fotohemolítica in vitro de Parthenium hysterophorus L. Revista Científica Villa Clara 16, 43–48.

Ugartondo, V., Mitjans, M., Vinardell, M.P., 2009. Applicability of lignins from different sources as antioxidants based on the protective effects on lipid peroxidation induced by oxygen radicals. Ind. Crop. Prod. 30, 184–187.

Van Elswijk, D.A., Schobel, U.P., Lansky, E.P., Irth, H., Van der Greef, J., 2004. Rapid dereplication of estrogenic compounds in pomegranate (*Punica granatum*) using on-line biochemical detection coupled to mass spectrometry. Phytochemistry 65, 233–241.

Vittori, D., Garbossa, G., Lafourcade, C., Pérez, G., Nesse, A., 2002. Human erythroid cells are affected by aluminium. Alteration of membrane band 3 protein. Biochim. Biophys. Acta Biomembr. 1558, 142–150.

Yang, H.-L., Chen, S.-C., Chang, N.-W., Chang, J.-M., Lee, M.-L., Tsai, P.-C., Fu, H.-H., Kao, W.-W., Chiang, H.-C., Wang, H.-H., Hseu, Y.-C., 2006. Protection from oxidative damage using Bidens pilosa extracts in normal human erythrocytes. Food Chem. Toxicol. 44, 1513–1521.